

# Biodiversity on island chains: neutral model simulations

Patrick B. Warren

Unilever R&D Port Sunlight, Bebington, Wirral, CH63 3JW, UK.

(Dated: April 6, 2010)

A neutral ecology model is simulated on an island chain, in which neighbouring islands can exchange individuals but only the first island is able to receive immigrants from a metacommunity. It is found by several measures that biodiversity decreases along the chain, being highest for the first island. Subtle changes in taxon abundance distributions can be detected when islands in the chain are compared to diversity-matched single islands. The results potentially apply to human microbial diversity, but highlight the difficulty of using static single-site taxon abundance distributions to discriminate between dispersal limitation mechanisms.

PACS numbers: 87.23.-n, 87.10.Mn, 02.50.Ga

It has recently been observed that human microbial diversity varies systematically between body sites [1, 2], for example phylogenetic diversity is higher for the palm of the hand and the sole of the foot, than for the armpit and forehead (Fig. S14 in Ref. 2). A high degree of inter-individual variability is also observed, to the point where the characterisation of residual skin bacteria has been proposed as a novel forensic tool [3]. The latter, in particular, supports the notion that *stochastic dispersal limitation* may play a significant role in determining microbial diversity. Stochastic dispersal limitation is a signature element of Hubbell's unified neutral model of biodiversity and biogeography [4], and this motivates the question of whether neutral models can be applied to human microbial biodiversity and biogeography. This is a hard problem and I do not claim to have solved it here. Rather, the present study is restricted to exploring the role of dispersal mechanisms in the context of neutral theory, keeping in mind the possible application to the human microbiome.

The merits of neutral models have been debated extensively [5], and it is far from obvious that they should apply to human microbiota [6, 7]. However Hubbell's neutral model has recently been successfully applied to predict microbial diversity in tree holes [8, 9]. In this context it is important to note that it has been argued dispersal limitation is the dominant factor determining taxon abundancies [10, 11], with other neutral model ideas, such as the zero-sum constraint (single trophic level; community saturation) or speciation by point mutation, playing a lesser role.

If taxon abundancies are largely determined by stochastic dispersal limitation, then a couple of limiting hypotheses (Fig. 1) present themselves to explain the observed variations in human microbial diversity. The first is a *variable-immigration-rate hypothesis* in which different body sites are envisaged as being microbial 'islands' in contact with a microbial metacommunity but effectively isolated from each other. Here variation in diversity corresponds to a variable immigration rate from the metacommunity. The second hypothesis is an *island-chain hypothesis* in which it is envisaged that migration can take place between islands but, *in extremis*, it is only

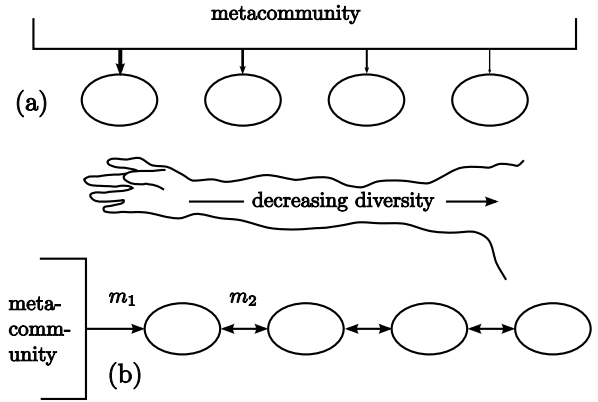


FIG. 1: Putative explanations for a variation in human microbial diversity, based on dispersal-limitation and the theory of island biogeography: (a) variable-immigration-rate hypothesis and (b) island-chain hypothesis.

the first island (*e.g.* the hand) that receives immigrants from the metacommunity. In this case one expects that diversity should decrease as one moves along the chain away from the island in contact with the metacommunity, due to dispersal limitation. This is confirmed in the present study.

Of course these hypotheses represent limiting cases and, if dispersal limitation is relevant, reality probably lies somewhere in between. A second question therefore is whether one can use taxon abundance distributions to distinguish between dispersal mechanisms. Unfortunately, the present study finds that both hypotheses lead to rather similar abundance distributions. When this is conflated with other factors, such as deviations from neutral model dynamics [12], it is probably going to be difficult to distinguish between dispersal mechanisms on the basis of static single-site measurements of microbial diversity.

The neutral model has been extensively studied for isolated islands in contact with a metacommunity [4, 10, 13–19], but only for certain cases has it been solved for multiple islands, or 'patches', which are able to exchange

individuals [20, 21]. In particular, the island chain problem has not been solved (*i. e.* where individuals can migrate between neighbouring islands but immigration is restricted to the first island in the chain). The primary goal of the present study is to solve this problem. Although in principle one can approach this analytically, the experience of Vallade and Houchmandzadeh [18] for *two* islands suggests this will be effectively unmanageable. I therefore approach the problem by means of simulations.

Let me start by summarising the mathematical characterisation of taxon abundance distributions. Suppose there are  $K$  taxa and  $N_i$  individuals in the  $i$ -th taxon ( $i = 1 \dots K$ ), in a population of  $J = \sum_{i=1}^K N_i$  individuals. The relative abundance of the  $i$ -th taxon is defined to be  $\omega_i = N_i/J$ . The taxon abundance distribution is characterised by  $\phi_k$ , the number of taxa containing  $k$  individuals. Formally  $\phi_k = \sum_{i=1}^K \delta_{k,N_i}$  where  $\delta_{n,m}$  takes the value unity if  $n = m$  and is zero otherwise. Given the set of  $N_i$  one can easily calculate  $\phi_k$ . One has  $K = \sum_{k=1}^{\infty} \phi_k$  and  $J = \sum_{k=1}^{\infty} k\phi_k$ . Since no taxon can contain more individuals than there are in the community as a whole,  $\phi_k = 0$  for  $k > J$ . Similarly  $\phi_J = 1$  if and only if all the individuals belong to the same taxon (the ‘monodominated’ state), otherwise  $\phi_J = 0$ .

In standard neutral model dynamics, population sizes remain fixed (saturated) and are specified at the outset, whilst the number of taxa and the number of individuals per taxon fluctuates. I adopt the notation of Vallade and Houchmandzadeh [13, 18] and write  $\langle \dots \rangle$  to indicate a quantity averaged over an ensemble of populations undergoing neutral model dynamics. The information in  $\langle \phi_k \rangle$  is conveniently represented by giving the ensemble-average probability  $p(\omega)$  that an individual belongs to a taxon of relative abundance  $\omega$  [13, 18, 22]. For a community of a finite size,  $p(\omega)$  is a discrete array or ‘comb’ of  $\delta$ -functions, even after ensemble-averaging, since  $\omega$  can only take on discrete multiples of  $1/J$ . However as  $J \rightarrow \infty$ ,  $p(\omega)$  becomes a continuous function. One can show that the continuum limit is  $p(\omega) = \lim_{J \rightarrow \infty} k \langle \phi_k \rangle$  where  $k = \omega J$  [13].

I shall additionally use several ensemble-average measures of diversity. The principal one of these is the Simpson diversity index [23], defined for a given set of taxon abundancies to be  $D = 1 - \sum_{i=1}^K \omega_i^2$ . It is related to the second moment of the taxon abundance distribution by  $D = 1 - J^{-2} \sum_{k=1}^{\infty} k^2 \phi_k$ . From this it can easily be shown that in the continuum limit

$$\langle D \rangle = 1 - \int_0^1 \omega p(\omega) d\omega. \quad (1)$$

The second diversity measure is the ensemble-average number of taxa  $\langle K \rangle = \sum_{k=1}^J \langle \phi_k \rangle$ . The third is the ensemble-average monodominance probability  $\langle \phi_J \rangle$ —as explained above  $\phi_J$  is 1 or 0 according to whether or not all the individuals belong to the same taxon.

As an order parameter, the Simpson index  $\langle D \rangle$  has some advantages over  $\langle K \rangle$  and  $\langle \phi_J \rangle$ : it remains well defined in the continuum limit  $J \rightarrow \infty$ , there are some

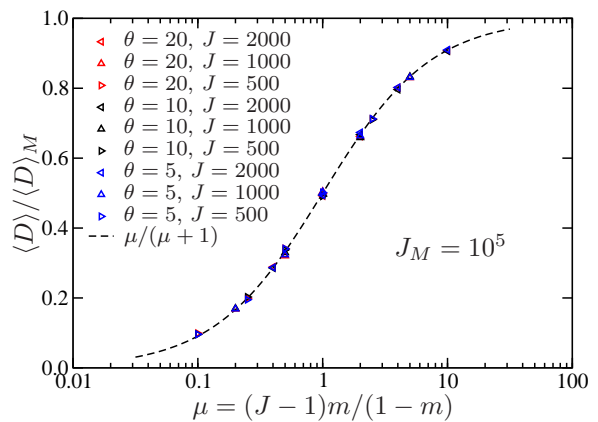


FIG. 2: Steady state island diversity  $\langle D \rangle$  from neutral model simulations on islands of various sizes with varying immigration rates, normalised by the metacommunity diversity  $\langle D \rangle_M = \theta/(\theta + 1)$ . The agreement with the theory, Eq. (7), is excellent. Error bars are smaller than the symbols.

particularly simple theoretical expressions for  $\langle D \rangle$  under neutral model dynamics, and in particular there is a prediction (confirmed by simulation) that  $\langle D \rangle$  factorises into a product of the metacommunity diversity index, and an island factor. Also the Simpson diversity index generalises naturally to a measure of  $\beta$ -diversity [20], and to time-series data [24]. The index satisfies  $0 \leq \langle D \rangle \leq 1 - 1/K$ . There is a mild disadvantage in that  $\langle D \rangle$  loses sensitivity to the underlying abundance distribution at the limiting values.

Let me next summarise neutral model dynamics. In the metacommunity it is as follows. An individual is selected at random, and with probability  $1 - \nu$  is replaced with a copy of another individual drawn at random from the metacommunity, or with probability  $\nu$  is replaced by an individual belonging to a new taxon. Thus  $\nu$  is the speciation rate. For  $\nu = 0$  the metacommunity eventually falls into a monodominated state, in an ecological analog of the Matthew principle [25]. For  $\nu > 0$  the taxon abundance distribution is a balance between speciation and extinction.

An explicit expression for the taxon abundance distribution in a metacommunity of size  $J_M$  has been obtained by a number of workers [4, 10, 13, 15–17]. Results are quoted as *metacommunity* (subscript ‘M’) steady-state ensemble-averages:

$$\langle \phi_k \rangle_M = \frac{\theta \Gamma(J_M + 1) \Gamma(J_M + \theta - k)}{k \Gamma(J_M + 1 - k) \Gamma(J_M + \theta)} \quad (2)$$

where  $\theta = (J_M - 1)\nu/(1 - \nu)$ . One has  $\theta \approx J_M \nu$  for  $J_M \gg 1$  and  $\nu \ll 1$ . It can be shown that  $\langle J \rangle_M = \sum_{k=1}^{J_M} k \langle \phi_k \rangle_M = J_M$  (an identity), and  $\langle K \rangle_M = \sum_{k=1}^{J_M} \langle \phi_k \rangle_M = \sum_{k=1}^{J_M} \frac{\theta}{\theta - 1 + k}$ . The continuum limit of Eq. (2) can be obtained using Stirling’s approximation. One finds  $p(\omega) = \theta(1 - \omega)^{\theta - 1}$ . It follows that the metacommunity diversity order parameter in the continuum

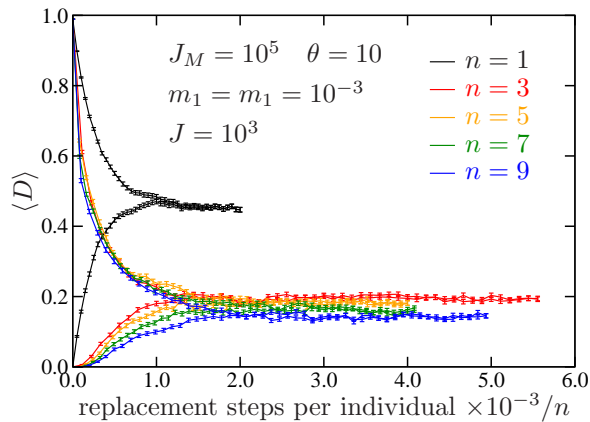


FIG. 3: Approach to steady state for the central island of a chain of length  $n$  islands starting from either a completely monodominated state (lower curves), or a flat abundance distribution (upper curves; flat means the  $N_i$  are equalised subject to  $\sum_{i=1}^K N_i = J$ ). The  $n = 1$  case is for a single island. For  $n > 1$  the steady state is weakly dependent on  $n$ .

limit is

$$\langle D \rangle_M = \frac{\theta}{\theta + 1}. \quad (3)$$

This result was noted by He and Hu by analogy to a similar problem in genetics [26].

Neutral model dynamics on an island connected to the metacommunity is as follows. An individual is selected at random, and with probability  $1 - m$  is replaced with a copy of another individual drawn at random from the island, or with probability  $m$  is replaced by an individual drawn at random from the metacommunity. Thus  $m$  is the immigration rate. Similar to the metacommunity, the island community eventually falls into a monodominated state if  $m = 0$ , whereas for  $m > 0$  a steady-state taxon abundance distribution arises as a balance between immigration and extinction. It is often a very good approximation to assume that the island dynamics are decoupled from the metacommunity dynamics; in other words the metacommunity can be taken to have a static abundance distribution. This is because the metacommunity abundance distribution turns over on a time scale of order  $1/\nu$  whereas the island abundance distribution turns over on a time scale of order  $1/m$ , and typically  $\nu \ll m$ . Here time scales are quoted in terms of the number of replacement steps per individual, since this is expected to be proportional to the real elapsed time [4].

Exact results for the island taxon abundance distribution were obtained only recently [10, 17], although partial results were obtained by previous authors [13–15]. The result is

$$\langle \phi_k \rangle = \binom{J}{k} \int_0^1 \frac{du}{u} \theta (1-u)^{\theta-1} \frac{(\mu u)_k (\mu(1-u))_{J-k}}{(\mu)_J} \quad (4)$$

where  $(x)_n = \Gamma(x+n)/\Gamma(x)$  is the Pochhammer symbol,  $\binom{J}{k} = \Gamma(J+1)/(\Gamma(k+1)\Gamma(J-k+1))$  is the bi-

nomial coefficient, and  $\mu = m(J-1)/(1-m)$  plays a role similar to  $\theta$  for the metacommunity. For  $J \gg 1$  and  $m \ll 1$ , one has  $\mu = Jm$ . Note that  $J_M$  does not feature in this expression, in other words the island abundance distribution is insensible to the metacommunity size. This point is discussed more thoroughly by Vallade and Houchmandzadeh [18]. Eq. (4) simplifies in the limit  $k = J$  to give an expression for the island monodominance probability,

$$\langle \phi_J \rangle = \int_0^1 \frac{du}{u} \theta (1-u)^{\theta-1} \frac{(\mu u)_J}{(\mu)_J}. \quad (5)$$

This depends strongly on all the relevant parameters and vanishes asymptotically for  $J \rightarrow \infty$  at fixed  $\mu$  as  $\langle \phi_J \rangle \sim \theta \Gamma(\theta) (\mu \ln J)^{-\theta}$ . The continuum limit of Eq. (4) is [10, 13, 17, 27]

$$p(\omega) = \mu \theta \int_0^1 \binom{\mu}{\mu u} (1-\omega)^{\mu u-1} \omega^{\mu(1-u)} u^\theta du. \quad (6)$$

Inserting Eq. (6) into Eq. (1) gives a simple but to my knowledge previously unreported result,

$$\langle D \rangle = \frac{\mu \theta}{(\mu + 1)(\theta + 1)}. \quad (7)$$

Remarkably, as alluded to above, the diversity index factorises into the product of the metacommunity diversity index  $\langle D \rangle_M = \theta/(\theta + 1)$  and an island factor  $\mu/(\mu + 1)$ .

Simulation of neutral model dynamics as summarised above is straightforward. I make the assumption that metacommunity and island dynamics are decoupled (discussed in more detail below). Therefore I generate a large number ( $10^3$ – $10^5$ ) of metacommunity abundance distribution samples for given  $J_M$  and  $\theta$ , equilibrating for  $10 \times J_M^2/\theta$  replacement steps between samples to ensure statistical independence [18]. I use these samples in subsequent island and island chain simulations. As a reference point, I shall use  $\theta = 10$ , motivated by Woodcock *et al.* [9], and  $J_M = 10^5$ , motivated not so much by time scale considerations (see later) but by the requirement that  $J_M \gg J \gg 1$  [18]. Except where otherwise stated, averages are over  $10^3$  samples.

I undertook a number of single island simulations to build confidence in the simulation and analysis methodologies. I find excellent agreement between these simulations and the theoretical predictions for the steady-state properties (equilibrating for  $10 \times J/m$  replacement steps between samples). For example Fig. 2 compares theory and simulation results for the Simpson diversity index.

The island chain simulations are performed similarly to the single island simulations. I introduce an immigration rate  $m_1$  (for the first island) and an inter-island migration rate  $m_2$ . This is illustrated in Fig. 1(b). Specifically, the dynamics are as follows. An individual is selected at random. If the chosen individual lies on the first island, it is replaced with a copy of another individual on the island with probability  $1 - m_1 - m_2$ , an immigrant from the

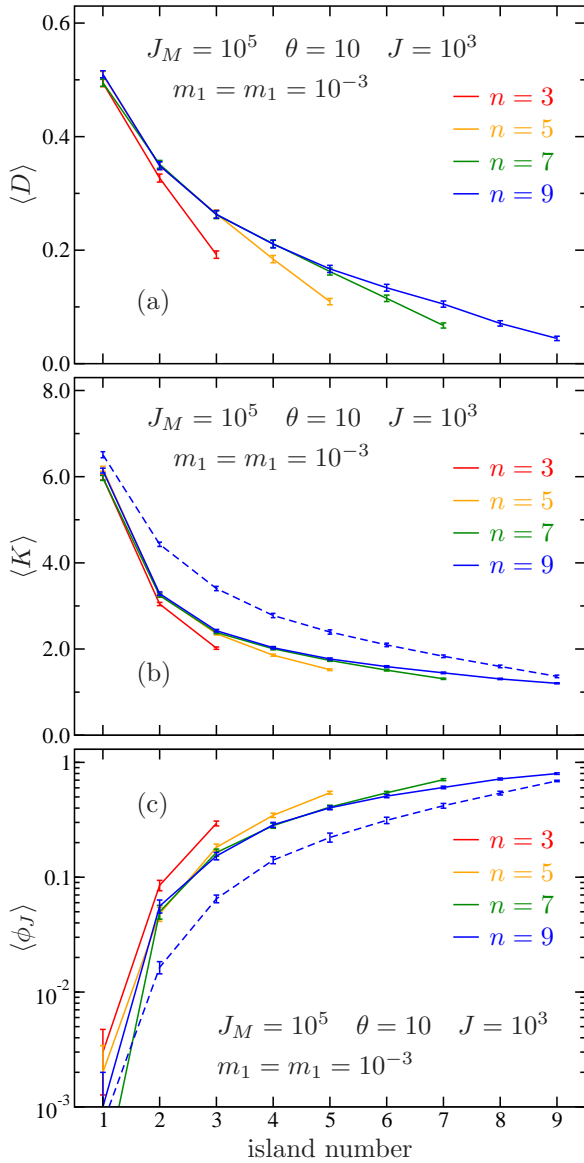


FIG. 4: Aspects of diversity on island chains of length  $n$ : (a) diversity index  $\langle D \rangle$ , (b) number of taxa  $\langle K \rangle$ , and (c) monodominance probability  $\langle \phi_J \rangle$ . The dashed lines in (b) and (c) are the  $\langle D \rangle$ -matched single island results for  $n = 9$  (see text).

metacommunity with probability  $m_1$ , or a migrant from the neighbouring island with probability  $m_2$ . If the chosen individual lies on an island interior to the chain, it is replaced with a copy of another individual on the island with probability  $1 - 2m_2$ , or with a migrant from one of the neighbouring islands (selected at random) with probability  $2m_2$ . If the chosen individual lies on the terminal island, it is replaced with a copy of another individual on the island with probability  $1 - m_2$ , or with a migrant from neighbouring island with probability  $m_2$ . Migrants are copies of individuals chosen at random on neighbouring islands.

Fig. 3 shows that the approach to steady state of a

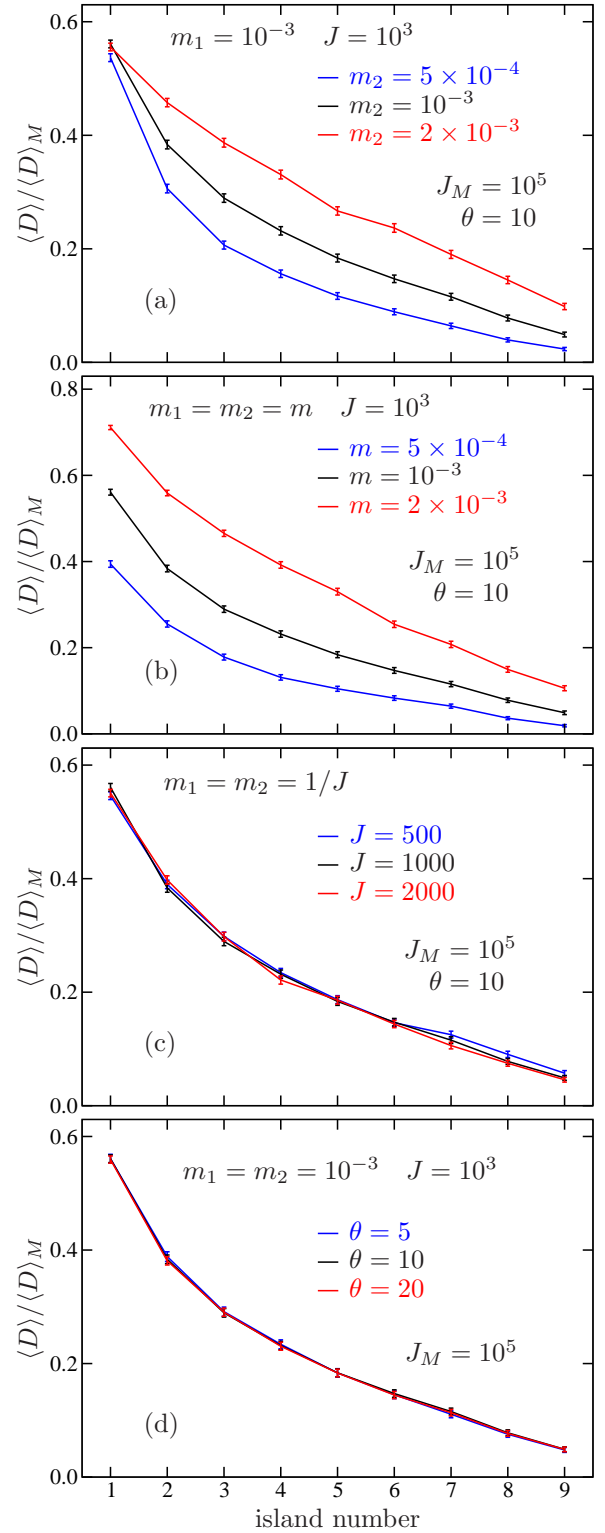


FIG. 5: Diversity index  $\langle D \rangle$ , normalised by the theoretical metacommunity diversity index  $\langle D \rangle_M = \theta/(\theta + 1)$ , along a chain of  $n = 9$  islands: (a) varying inter-island migration rate  $m_2$  only, (b) varying migration and immigration rates together at fixed island size, (c) varying migration and immigration rates inversely with island size, (d) varying metacommunity diversity parameter.

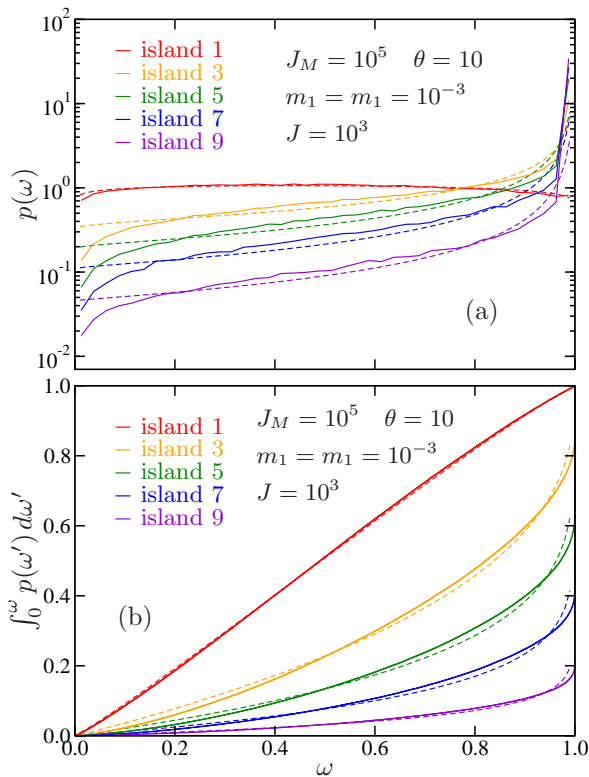


FIG. 6: Abundance distributions for selected islands in an island chain of length  $n = 9$ : (a) probability that a randomly selected individual belongs to a taxon of relative abundance  $\omega$ , and (b) cumulative distribution function of the same. The results (solid lines) are compared to the theoretical expectations for  $\langle D \rangle$ -matched single islands calculated from Eq. (6) (dashed lines). Results are averages over  $10^5$  samples.

chain of  $n$  islands is slowed by a factor  $\approx 1/n$  compared to the single island case. I therefore equilibrate the island chains against each metacommunity sample for at least  $10 \times n^2 J/m$  replacement steps between samples, where  $m$  is the smaller of  $m_1$  and  $m_2$ . In terms of the number of replacement steps per individual, the island chain relaxation time scale is of the order  $n/m$ . Clearly for  $n \gtrsim 10$  the assumed time scale separation between this and the metacommunity relaxation time  $1/\nu \approx J_M/\theta \approx 10^4$  is faltering. Nevertheless the results are still valid provided they can be shown to be unaffected by varying  $J_M$  since it can be assumed that in reality  $J_M$  is much larger than  $10^5$  [9]. To test this, I repeated many of the simulations with  $J_M = 5 \times 10^4$  and  $J_M = 2 \times 10^5$ . I found this made no difference to the measured island properties, within the statistical errors.

For a chain of length  $n = 9$ , I examined in some more detail how the islands recover their steady state diversity. The picture is a little mixed. The curves can be fitted by  $\langle D \rangle = A + B e^{-t/\tau}$ , but not very well, indicating there is not a clearly dominant relaxation time. Moreover the fitted value of  $\tau$  is affected by whether one starts with a monodominated state or a uniform state. What this all

suggests is that there is a spectrum of relaxation modes, which are excited differently according to the initialisation protocol, and which are subsequently mixed up by the non-linear dynamics. A more detailed exploration of this is left for future work.

Representative steady-state results for the island chain simulations are shown in Figs. 4–6. The first conclusion (Fig. 4) is that diversity decreases, by whatever measure, as one moves away from the island in contact with the metacommunity. Fig. 5 shows how island diversity varies with immigration and migration rates  $m_1$  and  $m_2$ , island size  $J$ , and the value of  $\theta$ . Increasing the inter-island migration rate  $m_2$  (Fig. 5(a)) has the effect of increasing the diversity along the island chain apart from the first island. Additionally increasing the metacommunity immigration rate  $m_1$  (Fig. 5(b)) leads to increased diversity along the whole chain. Fig. 5(c) supports the notion that the island diversity is governed by the combinations  $Jm_1$  and  $Jm_2$  rather than the individual values of  $J$ ,  $m_1$  and  $m_2$ , in close analogy to the theory for the single island. Similarly Fig. 5(d) strongly suggests that the Simpson diversity index continues to be factorisable into the metacommunity diversity index multiplied by a contribution from the structure of the island chain, again in close analogy to the single island result.

I next compare islands in the chain to ‘ $\langle D \rangle$ -matched’ single islands. Here  $\langle D \rangle$ -matching means a value for  $\mu$  is inferred from Eq. (7) (*i. e.*  $\mu = \langle D \rangle / (\langle D \rangle_M - \langle D \rangle)$  where  $\langle D \rangle_M = \theta / (\theta + 1)$ ), and used to calculate values of  $\langle K \rangle = \sum_{k=1}^J \langle \phi_k \rangle$  and  $\langle \phi_J \rangle$  from Eqs. (4) and (5). I assume the island size  $J$  is fixed. The procedure amounts to matching the first and second moments of  $\langle \phi_k \rangle$ . The dashed lines in Fig. 4(b) and (c) show systematically that the ensemble-average number of taxa is reduced and the monodominance probability is increased, comparing an island in the island chain with its  $\langle D \rangle$ -matched single island counterpart. Thus there is a tendency towards *fewer, larger taxa*, when islands in a chain are compared to  $\langle D \rangle$ -matched single islands.

A more detailed examination of the abundance distributions shows that there is a subtle and non-trivial redistribution of the taxon abundancies. When compared to the  $\langle D \rangle$ -matched single islands, Fig. 6 shows that  $p(\omega)$  is reduced for  $\omega \lesssim 0.2$  and  $\omega \gtrsim 0.8$ , but increased for  $0.2 \lesssim \omega \lesssim 0.8$ . This means that the number of taxa with intermediate abundancies is increased at the expense of the very rare taxa and the high abundance taxa. But, in addition, the cumulative distribution function jumps up at  $\omega = 1$ , as shown clearly in Fig. 6(b). This corresponds to the increased monodominance probability. At first sight this is at odds with with the redistribution towards mid-range abundancies, nevertheless it is a real effect and indeed is the reason why monodomination was separately studied.

The loss of the very rare taxa can perhaps be attributed to the filtering properties of the island chain. These taxa are already rare in the metacommunity and it could simply be that a representative from a rare taxon

is less likely to arrive via migration along an island chain than via direct immigration from the metacommunity (at matched  $\langle D \rangle$ ). The loss of the high abundance taxa and the increased monodominance probability are more mysterious and I do not at present have a clear mechanistic explanation. Possibly what is happening for islands in a chain, compared to  $\langle D \rangle$ -matched single islands, is that the monodominated state ( $\omega = 1$ ) has become ‘stickier’ in dynamical terms, without actually becoming an adsorbing state. In the monodominated state there is of course only one taxon, with  $\omega = 1$ , and this may come at the expense of the high abundance taxa with  $0.8 \lesssim \omega < 1$ .

For  $\langle D \rangle \lesssim 0.5$  the abundance distribution for a  $\langle D \rangle$ -matched *metacommunity* is almost exactly the same as that for a  $\langle D \rangle$ -matched single island. By this I mean that  $p(\omega) = \theta(1-\omega)^{\theta-1}$  with  $\theta = \langle D \rangle / (1 - \langle D \rangle)$  is a very good approximation to  $p(\omega)$  from Eq. (6). However a complete comparison with an equivalent metacommunity

is frustrated by the residual dependence of  $\langle K \rangle_M$  and  $\langle \phi_J \rangle_M$  on the metacommunity size  $J_M$ .

Despite these subtleties, it is clear from Fig. 6 that the taxon abundance distributions on an island chain are quite well approximated by  $\langle D \rangle$ -matched single islands. This is the origin of the claim in the introduction that it is probably going to be difficult to distinguish between dispersal mechanisms on the basis of static single-site measurements of the taxon abundancies. To resolve this question, or indeed to distinguish between dispersal-limitation and niche-adaptation [7], probably requires more detailed examination of the  $\beta$ -diversity [20, 21, 28], and dynamics [18, 19, 24]. In this context it may be useful to explore spatial correlations [20] and temporal correlations [24], which are natural generalisations of the Simpson index  $D$ .

I thank Mike Cates, Chris Quince, Bill Sloan, and Dave Taylor, for helpful comments.

- 
- [1] E. A. Grice, *et al.*, *Science* **324**, 1190 (2009).  
 [2] E. K. Costello, *et al.*, *Science* **326**, 1694 (2009).  
 [3] N. Fierer, *et al.*, *Proc. Natl. Acad. Sci. (USA)* (2010), doi:10.1073/pnas.1000162107.  
 [4] S. P. Hubbell, *The unified neutral theory of biodiversity and biogeography* (Princeton University press, Princeton, NJ, 2001).  
 [5] G. Bell, *Science* **293**, 2413 (2001); B. J. McGill, *Nature* **422**, 881 (2003); J. Chave, *Ecol. Lett.* **7**, 241 (2004); D. Alonso, R. S. Etienne, and A. J. McKane, *TRENDS Ecol. Evol.* **21**, 451 (2006); J. Chave, D. Alonso, and R. S. Etienne, *Nature* **441**, E1 (2006); E. G. Leigh, Jr., *J. Evol. Biol.* **20**, 2075 (2007).  
 [6] B. Foxman, *et al.*, *Interdisc. Perspect. Infect. Diseases* (2008), doi:10.1155/2008/613979.  
 [7] For human microbiota it seems quite likely that the most dominant taxa are niche-adapted, as for example *Staphylococcus epidermidis* on skin. However there is a large tail of rarer taxa for which dispersal limitation may be relevant.  
 [8] T. Bell, *et al.*, *Science* **308**, 1884 (2005); see also *Science* **309**, Letters (2005).  
 [9] S. Woodcock, *et al.*, *FEMS Microbiol. Ecol.* **62**, 171 (2007).  
 [10] R. S. Etienne and D. Alonso, *Ecol. Lett.* **8**, 1147 (2005).  
 [11] R. S. Etienne, D. Alonso, and A. J. McKane, *J. Theor. Biol.* **248**, 522 (2007).  
 [12] G. Bianconi, L. Ferretti, and S. Franz, *Europhys. Lett.* **87**, 28001 (2009).  
 [13] M. Vallade and B. Houchmandzadeh, *Phys. Rev. E* **68**, 061902 (2003).  
 [14] I. Volkov, *et al.*, *Nature* **424**, 1035 (2003).  
 [15] A. J. McKane, D. Alonso, and R. V. Solé, *Theor. Pop. Biol.* **65**, 67 (2004).  
 [16] F. He, *Functional Ecol.* **19**, 187 (2005).  
 [17] R. S. Etienne and D. Alonso, *J. Stat. Phys.* **128**, 485 (2006).  
 [18] M. Vallade and B. Houchmandzadeh, *Phys. Rev. E* **74**, 051914 (2006).  
 [19] P. Babak, *Phys. Rev. E* **74**, 021902 (2006).  
 [20] J. Chave and E. G. Leigh, Jr., *Theor. Pop. Biol.* **62**, 153 (2002).  
 [21] E. Condit, *et al.*, *Science* **295**, 666 (2002).  
 [22] The probability distribution function  $p(\omega)$  has also been advocated for the non-parametric Kolmogorov-Smirnov test to compare taxon abundance distributions; see J. C. Tipper, *Paleobiology* **5**, 423 (1979).  
 [23] E. H. Simpson, *Nature* **163**, 688 (1949).  
 [24] S. Azadeh, *et al.*, *Nature* **444**, 926 (2006).  
 [25] Matthew 25:29 (King James Version): “For unto every one that hath shall be given, and he shall have abundance: but from him that hath not shall be taken away even that which he hath.”.  
 [26] F. He and X.-S. Hu, *Ecol. Lett.* **8**, 386 (2005).  
 [27] D. Alonso and A. J. McKane, *Ecol. Lett.* **7**, 901 (2004).  
 [28] M. Dornelas, S. R. Connolly, and T. P. Hughes, *Nature* **440**, 80 (2006).